Investigation of Stimulated Polariton Scattering from the B_1-symmetry Modes of the KNbO$_3$ Crystal

Zhongyang Li[1]*, Mengtao Wang[1], Silei Wang[1], Bin Yuan[1], Pibin Bing[1], Degang Xu[2], and Jianquan Yao[2]

[1]College of Electric Power, North China University of Water Resources and Electric Power,
Zhengzhou, Henan 450045, China
[2]College of Precision Instrument and Opto-electronics Engineering, Institute of Laser
and Opto-electronics, Tianjin University, Tianjin 300072, China

Stimulated polariton scattering from the B_1-symmetry modes of a KNbO$_3$ crystal to generate a terahertz wave (THz-wave) with a noncollinear phase-matching scheme is investigated. The frequency-tuning characteristics of the THz-wave by varying the phase-matching angle and pump wavelength are analyzed. The expression for the effective parametric gain length under the noncollinear phase-matching condition is deduced. Parametric gain and absorption characteristics of the THz-wave in KNbO$_3$ are theoretically simulated. The characteristics of KNbO$_3$ for a terahertz parametric oscillator (TPO) are compared to those of MgO:LiNbO$_3$. The analysis indicates that KNbO$_3$ is an excellent optical crystal for a TPO, to enhance the THz-wave output.

Keywords : Stimulated polariton scattering, KNbO$_3$, Terahertz parametric oscillator
OCIS codes : (190.4410) Nonlinear optics, parametric process; (140.3070) Infrared and far-infrared lasers

I. INTRODUCTION

Over the past two decades, with the ever-increasing number of applications for terahertz (THz) radiation, such as imaging, biology, medicine, communications, security technologies, and quality control [1-6], there is growing demand for THz sources with excellent performance. Among many electronic and optical methods for terahertz-wave (THz-wave) generation, the terahertz parametric oscillator (TPO) [7] based on stimulated polariton scattering (SPS) processes exhibits many advantages, such as narrow linewidth, coherence, a wide tunable range, high power output, and room-temperature operation. A polariton is a coupled photon-phonon transverse-wave field, and polariton scattering is a nonlinear effect that occurs in crystals with both infrared- and Raman-active transverse optical (TO) modes [7]. In SPS, the interaction of a fundamental laser field with a polariton mode of a crystal generates a THz-wave and a Stokes wave. The wavelengths of the generated

THz-wave and Stokes wave depend on the phase-matching condition, giving rise to tunability. Typically the refractive index of the THz-wave is substantially larger than that for the optical-pump wave, and phase matching is impossible for collinear interactions. Noncollinear phase matching can perform well for THz generation [8-11]. One bonus of noncollinear phase matching is convenient frequency tuning of the THz-wave. However, the noncollinear phase-matching configuration, in which the pump, Stokes, and THz-waves are all not parallel to each other, significantly reduces parametric gain. Thus it is vitally important to increase the effective parametric gain length in the noncollinear phase-matching configuration.

A frequently employed material for TPOs is the nonlinear optical crystal MgO:LiNbO$_3$, because of its relatively large second-order optical nonlinearity and its wide transparency range [12]. Unfortunately, the quantum conversion efficiency of such a TPO is extremely low, as the THz-wave is intensely absorbed by the MgO:LiNbO$_3$ crystal. At a frequency of

Color versions of one or more of the figures in this paper are available online.

1.5 THz, the absorption coefficient is about 45 cm^{-1} [13]. $KNbO_3$ crystal is an attractive material for the nonlinear optical interaction between optical and THz-waves, due to its wide transmission range (0.4-4.5 μm) [14], high nonlinear coefficient ($d_{33} = 27.4$ pm/V at 1064 nm) [15], and relatively high optical-damage threshold of 350 MW/cm^2 [16]. $KNbO_3$ has four infrared- and Raman-active TO phonon modes, called B_1-symmetry modes, located at 187, 243, 270, and 534 cm^{-1} [17]. When pump excitation is sufficiently strong, a THz-wave can be generated from the efficient parametric scattering of laser light via SPS.

In this Letter, we theoretically study the characteristics of $KNbO_3$ for a TPO with a noncollinear phase-matching scheme. We analyze the frequency-tuning characteristics of the THz-wave by varying the phase-matching angle and pump wavelength. The expression of the effective parametric gain length under the noncollinear phase-matching condition is deduced. The gain and absorption characteristics of THz-waves in $KNbO_3$ and $MgO:LiNbO_3$ are investigated.

II. THEORETICAL MODEL

A surface-emitting TPO with a noncollinear phase-matching scheme comprises a single-resonant optical parametric oscillator with a Fabry-Perot cavity, as shown in Fig. 1. The configuration was first reported by T. Ikari *et al*. [18]. The nonlinear optical crystal is $KNbO_3$. The resonant cavity for the Stokes wave consists of two plane-parallel mirrors M_1 and M_2 of high reflectance. The pump wave passes through the cavity at the edges of M_1 and M_2, and the Stokes wave propagates along the x-axis of the $KNbO_3$. A THz-wave vector perpendicular to the output surface is achieved by setting the angle of incidence of the pump wave to the crystal surface. The polarizations of the pump, Stokes, and THz-waves are all along the z-axis of the $KNbO_3$ crystal. θ is the angle between the vectors of the pump and Stokes waves within the crystal, and φ is the angle between the vectors of the pump and THz-waves within the crystal. The cavity mirrors and $KNbO_3$ crystal are mounted on a rotating stage. The wavelength of the Stokes wave, and hence the wavelength of the THz-wave, can be tuned by rotating the stage continuously, since that changes the angle θ continuously.
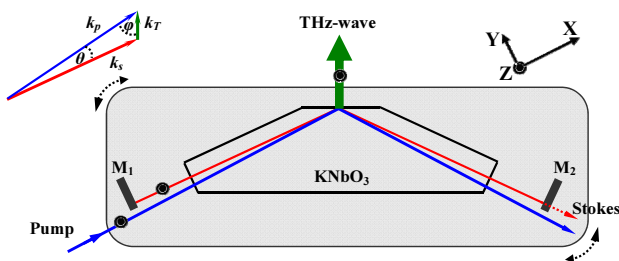

FIG. 1. Schematic diagram of a surface-emitting TPO using $KNbO_3$ with a noncollinear phase-matching scheme.

The theoretical values of refractive index are calculated using the Sellmeier equation for $KNbO_3$ in the infrared range at 22°C [14] and in the THz range [17], respectively. In this Letter, the theoretical parameters for $KNbO_3$ are taken from reference [17].

III. TUNING CHARACTERISTICS

For tunable THz-wave generation, two requirements must be fulfilled: the energy conservation law $\omega_p = \omega_s + \omega_T$, and the noncollinear phase-matching condition $\boldsymbol{k}_p = \boldsymbol{k}_s + \boldsymbol{k}_T$, as shown in the inset of Fig. 1. Here, ω_p, ω_s and ω_T are the angular frequencies, while $\boldsymbol{k}_p$, $\boldsymbol{k}_s$ and $\boldsymbol{k}_T$ are the wave-vectors of the pump, Stokes and THz-wave, respectively. The phase matching condition can be rewritten as $k_T^2 = k_p^2 + k_s^2 - 2k_p^2 k_s^2 \cos\theta$. By varying one parameter of the noncollinear phase-matching condition, such as the angle θ or the pump wavelength λ_p, we can obtain a family of phase-matching curves. Figure 2 shows the dispersion curve of the B_1-symmetry polariton modes in $KNbO_3$ and the phase-matching curves for the 1064-nm laser pump. When the phase-matching curves are superimposed on the dispersion curve of the B_1-symmetry polariton modes, the points of intersection of these curves are expected to determine the allowed frequencies and wave vectors of the THz wave. As the angle θ is changed continuously, the frequency tuning of the THz wave is realized simultaneously, which is the basic principle of the so-called angle-tuning method for a TPO. When the angle θ varies from 0° to 7.3°, the phase-matching curves and the dispersion curve of the B_1-symmetry polariton modes intersect, which means a THz-wave can be generated.

According to the noncollinear phase-matching condition, tuning of a THz-wave can be realized by varying the pump wavelength λ_p. Figure 3 shows the dispersion curve of the B_1-symmetry polariton modes in $KNbO_3$ and the
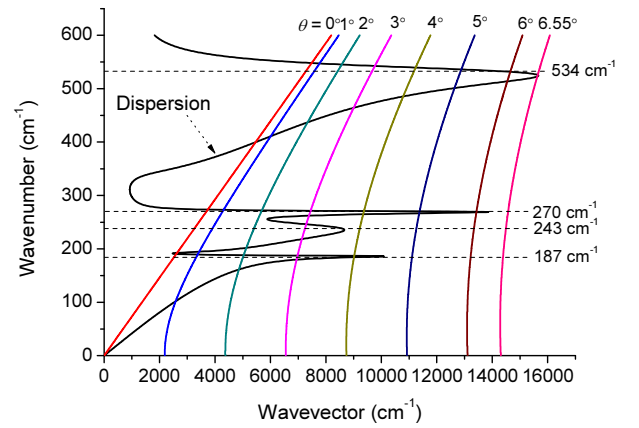

FIG. 2. Dispersion curve for the B_1-symmetry polariton modes in $KNbO_3$ and the phase-matching curves for the 1064-nm pump laser.
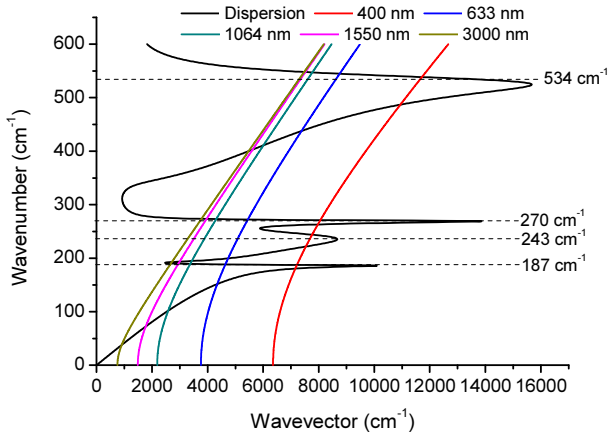
FIG. 3. Dispersion curve for the B_1-symmetry polariton modes in KNbO$_3$ and the phase-matching curves, at room temperature and a fixed phase-matching angle θ of 1°.

phase-matching curves at a fixed phase-matching angle θ of 1°, when the pump wavelengths are 400, 633, 1064, 1550, and 1064 nm respectively. From the figure we find that when the pump wavelength λ_p changes, the intersection points of the phase-matching curves and the dispersion curve of the B_1-symmetry polariton modes change, which means that frequency tuning of the THz wave is realized simultaneously. The shorter the pump wavelength, the higher the frequency shift of the intersection point; that is, a higher-frequency THz-wave will be achieved.

IV. EFFECTIVE PARAMETRIC GAIN LENGTH CHARACTERISTICS

The effective parametric gain length is of vital importance for THz-wave output, as the noncollinear phase-matching scheme is employed in the TPO. Next we deduce the expression for the effective parametric gain length under the noncollinear phase-matching condition, based on the theoretical model proposed in Ref. [19]. In this Letter we regard the phase-matching angle θ between the vectors of the pump and Stokes waves as a double refraction walkoff angle, since the magnitudes of both angles are approximately equal, and the effect of both is identical. Assuming the three mixing waves have Gaussian profiles, the Stokes spot size is simultaneously narrowed by gain polarization and broadened by diffraction. The balance determines the final Stokes-wave spot size. The relationship between the pump-wave radius w_p and the Stokes-wave radius w_s is given by

$$\left(\frac{\pi}{2L\lambda_s}\right)^2\left(\frac{w_p^2 w_s^2}{w_p^2+2w_s^2}\right)^3+\frac{w_p^2 w_s^2}{w_p^2+2w_s^2}-\frac{w_p^2}{2}=0 \tag{1}$$

where λ_s is the wavelength of the Stokes wave and L is the optical cavity's length. The walkoff length l_ω is given by
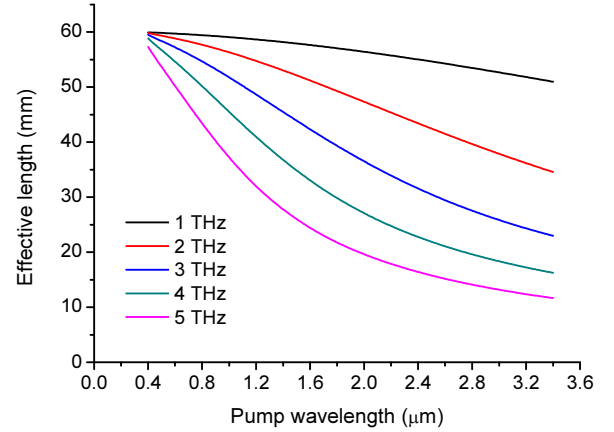

FIG. 4. Effective parametric gain length versus pump wavelength, assuming the physical length of the resonant cavity is 80 mm, l is 60 mm, and w_p is 1 mm.

$$l_\omega = \frac{\sqrt{\pi}}{2}\frac{w_p}{\theta}\left(\frac{w_p^2+w_s^2}{w_p^2+w_s^2/2}\right)^{\frac{1}{2}} \tag{2}$$

where θ is used as a substitute for the double refraction walkoff angle. The effective parametric gain length L_{eff} is given by

$$L_{eff} = l_\omega\, erf\left(\frac{\sqrt{\pi}}{2}\frac{l}{l_\omega}\right) \tag{3}$$

where l is the crystal's length, which is the propagation length of the Stokes wave within the KNbO$_3$ crystal. The effective parametric gain length L_{eff} versus the pump wavelength λ_p is shown in Fig. 4, when the frequency of the THz-wave equals 1, 2, 3, 4, and 5 THz respectively. From the figure we find that as the pump wavelength increases, the effective parametric gain length gradually decreases. The reason is that as the pump wavelength increases, the phase-matching angle θ is enlarged. The pump wave in the short-wavelength region can effectively lengthen the effective parametric gain length. Compared to frequencies of 2, 3, 4, and 5 THz, the effective parametric gain length is maximal at a THz-wave frequency of 1 THz, because the phase-matching angle θ is minimal at 1 THz.

Figure 5 shows the effective parametric gain length versus the radius of the pump wave, when the frequency of the THz-wave is 1, 2, 3, 4, and 5 THz respectively. From the figure we find that the effective parametric gain length increases rapidly and smoothly with increasing pump-wave radius. A pump wave with a large beam radius can generate a Stokes wave and a THz-wave with a large beam radius simultaneously, resulting in a long effective parametric gain length. Actually, for maximum conversion efficiency the pump beam diameter must be increased until the effective parametric gain length is equal to the crystal's length.
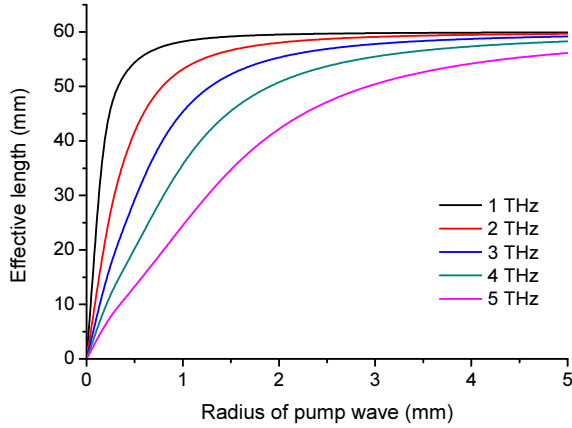
FIG. 5. Effective parametric gain length versus the radius of the pump wave, assuming the physical length of the resonant cavity is 80 mm, l is 60 mm, and λ_p is 1064 nm.
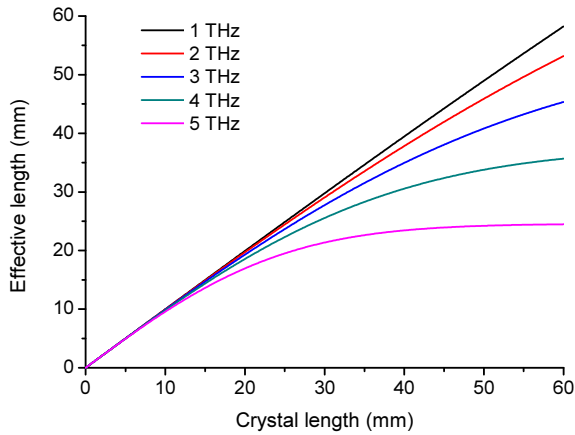

FIG. 6. Effective parametric gain length versus crystal length, assuming the physical length of the resonant cavity is 80 mm, w_p is 1 mm, and λ_p is 1064 nm.

Figure 6 shows the effective parametric gain length versus crystal length, when the frequency of THz-wave is 1, 2, 3, 4, and 5 THz respectively. From the figure we find that the effective parametric gain length increases rapidly with increasing crystal length for frequencies of 1, 2, and 3 THz, and increases smoothly as the frequency climbs to 4 and 5 THz. At lower frequencies of the THz-wave, the pump and Stokes waves almost overlap, as the phase-matching θ is small. On the contrary, the pump and Stokes waves separate rapidly, as the two beams only partially overlap at higher frequencies.

V. GAIN AND ABSORPTION CHARACTERISTICS

For efficient generation of the THz-wave, parametric gain is another crucial parameter. According to Ref. [20], the analytical expression for the THz-wave parametric gain g_T under the noncollinear phase-matching condition can be written as

$$g_T = \frac{\alpha_T}{2}\left\{\left[1+16\cos\varphi\left(\frac{g_0}{\alpha_T}\right)^2\right]^{\frac{1}{2}}-1\right\} \quad (4)$$

$$g_0^2 = \frac{\pi\omega_s\omega_T}{2c^3 n_p n_s n_T}I_p\left(d'_E + \sum_j \frac{S_j\omega_{0_j}^2 d'_{Q_j}}{\omega_{0_j}^2 - \omega_T^2}\right)^2 \quad (5)$$

$$\alpha_T = 2\frac{\omega_T}{c}\text{Im}\left(\varepsilon_\infty + \sum_j \frac{S_j\omega_{0_j}^2}{\omega_{0_j}^2 - \omega_T^2 - i\omega_T\Gamma_j}\right)^{\frac{1}{2}} \quad (6)$$

where α_T is the absorption coefficient in the THz region, ω_{0_j}, S_j and Γ_j respectively denote the eigenfrequency, oscillator strength of the polariton modes, and bandwidth of the jth B₁-symmetry phonon mode in the KNbO₃ crystal. I_p is the power density of the pump wave, and g_0 is the low-loss parametric gain. n_p and n_s are the refractive indices of the pump and Stokes waves respectively. d'_E and d'_Q are the nonlinear coefficients related to pure parametric (second-order) and Raman (third-order) scattering processes respectively. Far below the lowest B₁-symmetry polariton mode at 187 cm⁻¹, Eq. (5) can be rewritten as

$$g_0^2 = \frac{\pi\omega_s\omega_T}{2c^3 n_p n_s n_T}I_p\left(d'_E + \sum_j S_j d'_{Q_j}\right)^2 \quad (7)$$

The nonlinear coefficients d'_E and d'_Q relate to the electro-optic coefficient r:

$$d'_E + \sum_j S_j d'_{Q_j} = rn_T^4 \quad (8)$$

Thus the low-loss parametric gain coefficient g_0 is rewritten as

$$g_0^2 = \frac{\pi\omega_s\omega_T}{2c^3 n_p n_s n_T}I_p\left(rn_T^4\right)^2 \quad (9)$$

According to Eqs. (4)~(9), we plot the parametric gain coefficient g_T at a pump intensity of 100 MW/cm² and the absorption coefficient α_T in KNbO₃ and MgO:LiNbO₃, as shown in Figs. 7(a) and 7(b) respectively. From the figure we find that, as the frequency of the THz-wave is far below the lowest B₁-symmetry polariton mode at 187 cm⁻¹, the values of the parametric gain coefficient g_T for KNbO₃ and MgO:LiNbO₃ are of the order of several cm⁻¹. The gain coefficient of KNbO₃ is larger than that of MgO:LiNbO₃. Meanwhile, the values of the absorption coefficient α_T of the THz-wave in KNbO₃ are much smaller than those of MgO:LiNbO₃. Compared to MgO:LiNbO₃, KNbO₃ has a
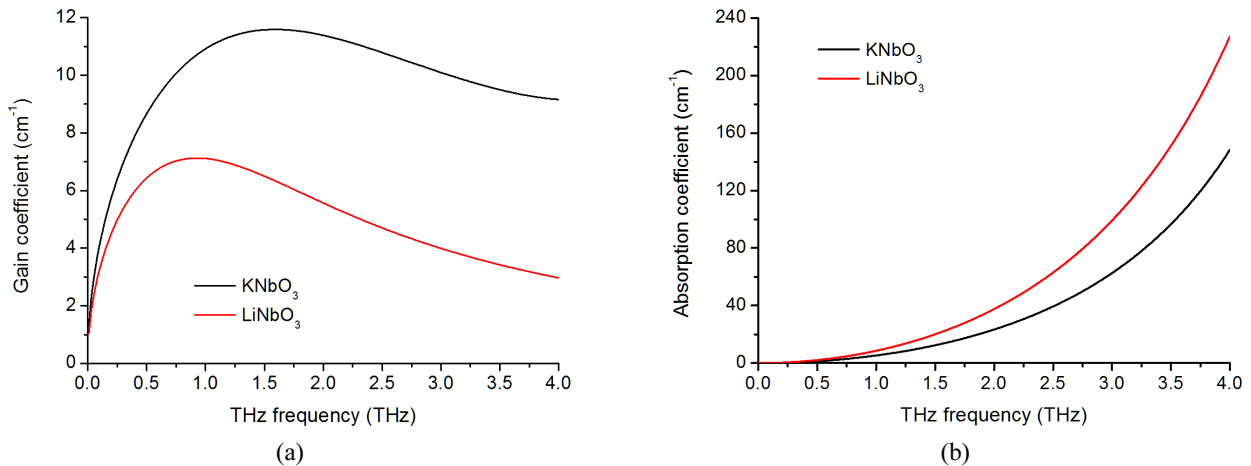
FIG. 7. THz-wave parametric gain coefficient g_T and absorption coefficient α_T for KNbO$_3$ and MgO:LiNbO3 at room temperature ($\lambda_p = 633$ nm, $I_p = 100$ MW/cm^2): (a) gain coefficient g_T, (b) absorption coefficient α_T.

larger gain coefficient and smaller absorption coefficient, so KNbO$_3$ is a more suitable selection for a TPO to enhance THz-wave output.

VI. CONCLUSION

SPS from the B$_1$-symmetry modes of KNbO$_3$ crystal to generate a THz-wave with a noncollinear phase-matching scheme is investigated. A widely tunable THz-wave can be generated by varying the phase-matching angle and pump wavelength. A pump wave with shorter wavelength and larger beam radius can significantly increase the effective parametric gain length under the noncollinear phase-matching condition. Compared to MgO:LiNbO$_3$, KNbO$_3$ has a larger gain coefficient and smaller absorption coefficient, so KNbO$_3$ is an excellent optical crystal for a TPO.

ACKNOWLEDGEMENT

REFERENCES

1. L. Ho, M. Pepper, and P. Taday, "Terahertz spectroscopy: Signatures and fingerprints," Nat. Photon. **2**, 541-543 (2008).
2. D. Abbott and X. C. Zhang, "Scanning the issues: T-ray imaging, sensing, and retection," Proc. IEEE **95**, 1509-1513 (2007).
3. J. L. Liu, J. M. Dai, S. L. Chin, and X. C. Zhang, "Broadband terahertz wave remote sensing using coherent manipulation of fluorescence from asymmetrically ionized gases," Nat. Photon. **4**, 627-631 (2010).
4. T. Kleine-Ostmann and T. Nagatsuma, "A review on terahertz communications research," J. Infrared, Millimeter, Terahertz Waves **32**, 143-171 (2011).
5. M. Tonouchi, "Cutting-edge terahertz technology," Nat. Photon. **1**, 97-105 (2007).
6. D. Bigourd, A. Cuisset, F. Hindle, S. Matton, E. Fertein, R. Bocquet, and G. Mouret, "Detection and quantification of multiple molecular species in mainstream cigarette smoke by continuous-wave terahertz spectroscopy," Opt. Lett. **31**, 2356-2358 (2006).
7. K. Kawase, J. Shikata, and H. Ito, "Terahertz wave parametric source," J. Phys. D: Appl. Phys. **35**, R1-R14 (2002).
8. D. Wu and T. Ikari, "Enhancement of the output power of a terahertz parametric oscillator with recycled pump beam," Appl. Phys. Lett. **95**, 141105 (2009).
9. Y. J. Ding, "High-power tunable terahertz sources based on parametric processes and applications," IEEE J. Sel. Topics Quantum Electron. **13**, 705-720 (2007).
10. T. Ikari, R. Guo, H. Minamide, and H. Ito, "Energy scalable terahertz-wave parametric oscillator using surface-emitted configuration," J. Eur. Opt. Soc. **5**, 10054 (2010).
11. Y. J. Ding and W. Shi, "From backward THz difference-frequency generation to parametric oscillation," IEEE J. Sel. Topics Quantum Electron. **12**, 352-359 (2006).
12. R. Sowade, I. Breunig, C. Tulea, and K. Buse, "Nonlinear coefficient and temperature dependence of the refractive index of lithium niobate crystals in the terahertz regime," Appl. Phys. B **99**, 63-66 (2010).
13. D. Molter, M. Theuer, and R. Beigang, "Nanosecond terahertz optical parametric oscillator with a novel quasi phase matching scheme in lithium niobate," Opt. Express **17**, 6623-6628 (2009).
14. B. Zysset, I. Biaggio, and P. Günter, "Refractive indices of orthorhombic KNbO$_3$. I. Dispersion and temperature

dependence," J. Opt. Soc. Am. B **9**, 380-386 (1992).

15. I. Biaggio, P. Kerkoc, L. S. Wu, P. Günter, and B. Zysset, "Refractive indices of orthorhombic KNbO$_3$. II. Phase-matching configurations for nonlinear-optical interactions," J. Opt. Soc. Am. B **9**, 507-517 (1992).

16. W. Seelert, P. Kortz, D. Rytz, B. Zysset, D. Ellgehausen, and G. Mizell, "Second-harmonic generation and degradation in critically phase-matched KNbO$_3$ with a diode-pumped Q-switched Nd:YLF laser," Opt. Lett. **17**, 1432-1434 (1992).

17. D. G. Bozinis and J. P. Hurrell, "Optical modes and dielectric properties of ferroelectric orthorhombic KNbO$_3$,"

Phys. Rev. B **13**, 3109-3120 (1976).

18. T. Ikari, X. Zhang, H. Minamide, and H. Ito, "THz-wave parametric oscillator with a surface-emitted configuration," Opt. Express **14**, 1604-1610 (2006).

19. S. J. Brosnan and R. L. Byer, "Optical parametric oscillator threshold and linewidth studies," IEEE J. Quantum Electron. **15**, 415-431 (1979).

20. S. S. Sussman, *Tunable Light Scattering from Transverse Optical Modes in Lithium Niobate* (Microwave Laboratory Report No. 1851, Stanford University, 1970), pp. 22-52.